

16 channel 200 GHz arrayed waveguide grating based on Si nanowire waveguides*

Zhao Lei(赵雷), An Junming(安俊明)[†], Zhang Jiashun(张家顺), Song Shijiao(宋世娇),
Wu Yuanda(吴远大), and Hu Xiongwei(胡雄伟)

State Key Laboratory of Integrated Optoelectronics, Institute of Semiconductors, Chinese Academy of Sciences,
Beijing 100083, China

Abstract: A 16 channel arrayed waveguide grating demultiplexer with 200 GHz channel spacing based on Si nanowire waveguides is designed. The transmission spectra response simulated by transmission function method shows that the device has channel spacing of 1.6 nm and crosstalk of 31 dB. The device is fabricated by 193 nm deep UV lithography in silicon-on-substrate. The demultiplexing characteristics are observed with crosstalk of 5–8 dB, central channel's insertion loss of 2.2 dB, free spectral range of 24.7 nm and average channel spacing of 1.475 nm. The cause of the spectral distortion is analyzed specifically.

Key words: integrated optics; arrayed waveguide grating; Si nanowire waveguides

DOI: 10.1088/1674-4926/32/2/024010

EEACC: 4140

1. Introduction

In the past decade, the demands for communication services have exploded, which has impelled the prosperous development of the high-speed and large-capability optical networks. Among the different kinds of the optical components, the planar light wave circuit type is always the focus because of its excellent characteristic, such as low cost, small size, high stability and mass-producibility. With the trends towards the high density photonic integrated circuits, silicon-on-insulator (SOI) substrate, which is compatible with the complementary metal–oxide–semiconductor technology, has attracted many researchers^[1–5]. The typical characteristic of SOI substrate is the ultra-high refractive index difference, so the submicron waveguide has strong confinement and can allow very sharp bends with low radiation losses. Thus, the photonic devices based on SOI can minimize their sizes to the order of mm² or μm². Currently, arrayed waveguide grating (AWG) is a crucial component for wavelength division multiplexing (WDM) systems^[6,7], and the studies on ultrasmall AWG with broad channel spacing have been reported^[8,9]. In this paper, we present a design of the large port number and narrow channel spacing AWG based on Si nanowire waveguides and analyze the measured results in detail.

2. Design

The SOI wafer in this paper is with 220 nm top Si layer and 2 μm buried oxide (BOX) layer. Due to the serious polarization-sensitive of Si nanowire, our device is designed for operating at the transverse-electric (TE) mode. In the device, all the waveguides are channel waveguides and the single mode condition are calculated with the FimmWAVE software from PhotonDesign Company. To the nanowire waveguides, the propagation loss is dominated by the scattering loss which

comes from the roughness of the waveguide sidewall. For the propagation loss increases quickly with the reduction of the waveguide width, the waveguide width needs an appropriate value, and thus 500 nm is chosen.

Light propagation in the AWG must satisfy the grating equation:

$$n_s d \sin \theta_i + n_c d \sin \theta_o + n_c \Delta L = m \lambda, \quad (1)$$

where n_s and n_c are the effective refractive index of the slab and channel waveguides, d is the grating pitch, θ_i and θ_o are the diffraction angles at the input and output slabs, ΔL is the constant path difference between neighboring waveguides in the arrayed waveguide region, and m is the diffraction order. When $\theta_i = \theta_o = 0$, the central wavelength λ_0 of the array is defined as

$$n_c \Delta L = m \lambda_0. \quad (2)$$

The relationship between the free spectral range (FSR) and the diffraction order is given as

$$\text{FSR} = N \Delta \lambda = \frac{\lambda_0 n_c(\lambda)}{m n_g(\lambda)}, \quad (3)$$

where $\Delta \lambda$ is the channel spacing, n_c , n_g is the effective index and the group index of the channel waveguides, and N is the number of the input (output) channels. From Eq. (3), the maximum value of the diffraction order can be calculated.

By differentiating equation (1), the spectral dispersion can be obtained as

$$\frac{d\theta}{d\lambda} = \frac{m n_g}{n_s d n_c}. \quad (4)$$

Then the channel spacing can be acquired from the spectral

* Project supported by the National High Technology Research and Development Program of China (No. 2006AA03Z420) and the National Natural Science Foundation of China (Nos. 60776057, 60837001, 60776057).

[†] Corresponding author. Email: junming@semi.ac.cn

Received 7 July 2010, revised manuscript received 8 September 2010

© 2011 Chinese Institute of Electronics

Table 1. Design parameters of Si nanowire AWG.

Parameter	Value
Central wavelength λ_0	1552 nm
Channel spacing $\Delta\lambda$	1.6 nm
Number of I/O channels N	16
I/O channels separation $\Delta x_i(0)$	1.5 μm
Grating pitch d	1 μm
Diffraction order m	37
Length difference of adjacent waveguides ΔL	23.5 μm
Focal length of the slab waveguide R	44.1 μm
Free spectral range (FSR)	25.6 nm
Number of arrayed waveguides	42

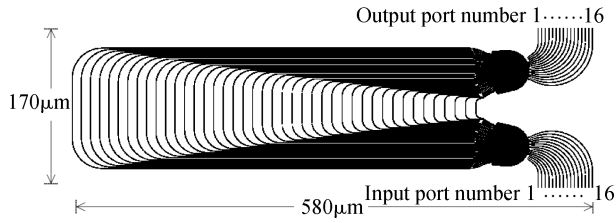


Fig. 1. Schematic of AWG based on Si nanowire waveguides.

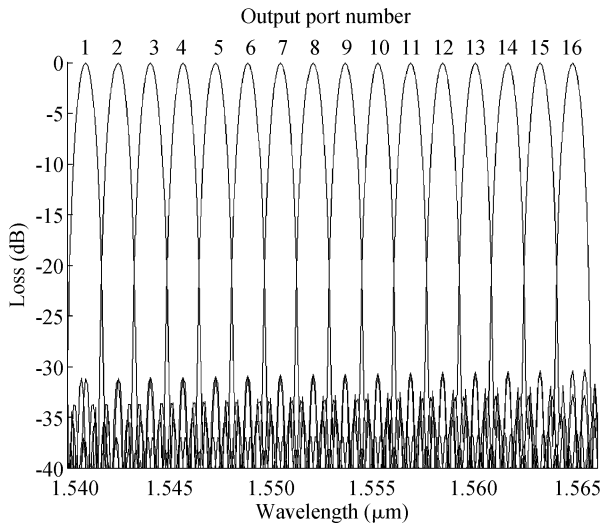
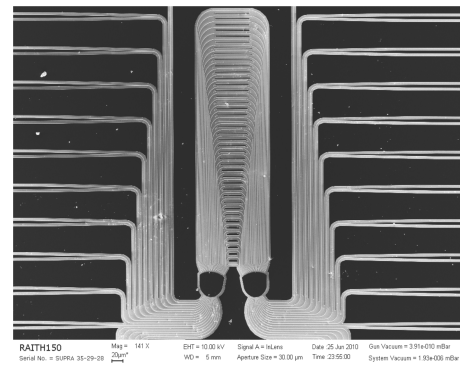


Fig. 2. Simulated transmission spectra of AWG based on Si nanowire waveguides from eleventh input port.

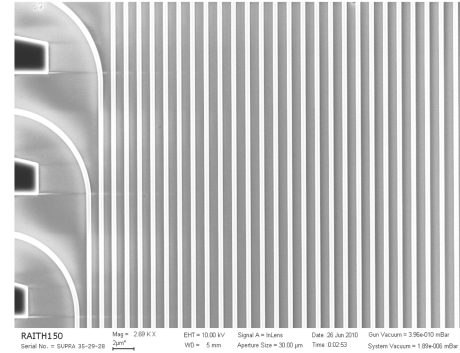
dispersion, as follows:

$$\begin{aligned} \Delta\lambda &= \Delta\theta \left(\frac{d\theta}{d\lambda} \right)^{-1} = \Delta\theta \frac{n_s d}{m} \left(\frac{n_g}{n_c} \right)^{-1} \\ &= \frac{\Delta x_0 n_s d}{R m} \left(\frac{n_g}{n_c} \right)^{-1}, \end{aligned} \quad (5)$$

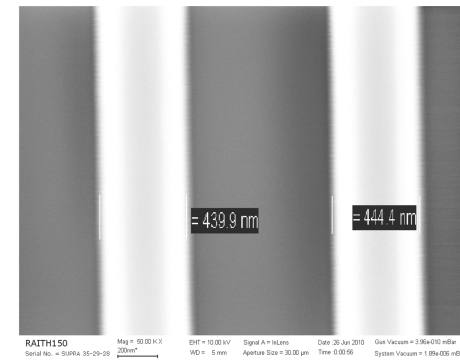
where Δx_0 is the output channels separation, and R is the focal length of the slab waveguide. According to Eqs. (2), (3) and (5), the main parameter of AWG can be fixed. The design parameters of Si nanowire AWG are given in Table 1 and the schematic is shown in Fig. 1.



(a)



(b)



(c)

Fig. 3. SEM of fabricated AWG based on Si nanowire waveguides. (a) Top view. (b), (c) Enlarged view of the waveguide in the arrayed waveguide region.

3. Simulation and test

The transmission spectra of AWG is simulated by a transmission function method, and Figure 2 shows the simulation results of the 16 output ports as a function of the wavelength from the eleventh input port. The simulated central wavelength and channel spacing are consistent with the design values, and the crosstalk is 31 dB.

The designed AWG is fabricated with a high-quality fabrication tool, 193 nm deep UV lithography, which is used for advanced complementary metal-oxide-semiconductor fabrication. Figure 3 shows SEM pictures of the fabricated AWG. After chip dicing and facet polishing, an amplified spontaneous emission source with a spectrum range of 1530–1610 nm and an optical spectrum analyzer are used to characterize the device. Polarizer and polarization maintaining fiber are com-

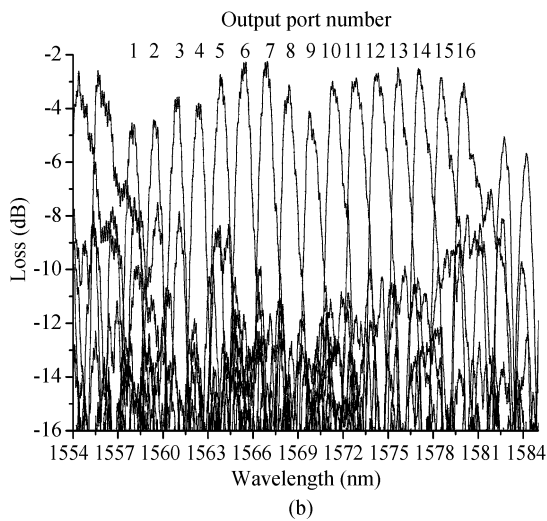
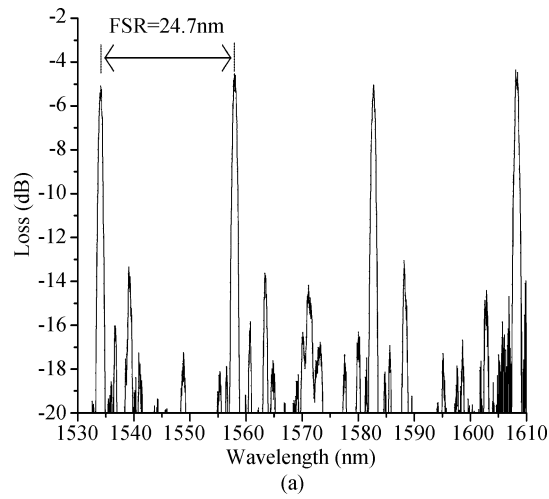


Fig. 4. Measured transmission spectra of fabricated AWG from eleventh input port. (a) First output port. (b) All output ports.

bined to get the TE-polarization light to enter the eleventh input port. Figure 4 shows the measured spectral response which is normalized to the spectral response of a simple nanowire waveguide. The crosstalk of the adjacent channels is 13 dB in Fig. 4(a). The factor dominating the crosstalk is the phase noise in the arrayed region, which is from the bad uniformity linewidth and the scattering on the rough core-cladding interface. The general crosstalk is between 5 dB and 8 dB in Fig. 4(b). The degradation of the general crosstalk is from the tenth to the sixteenth output ports. For the different output ports, all the parameters are the same except the channel separation. The displacement of the channel separation in the tenth-sixteenth output ports induce the other channel's wavelength entering the measured channel, so the final spectrum fluctuates. For the central output ports, the insertion loss is 2.5 dB. The nonuniformity between central and outer ports is 2.2 dB. The free spectral range (FSR) is 24.7 nm and the average channel spacing is 1.475 nm. The reduction of these two parameters is related with the decrease in the waveguide width. With the waveguide width diminishing, the ratio of the effective index n_c with the group index n_g is also shrinking. Figure 5 shows the relationship of the ratio n_c/n_g and waveguide width. When the channel spacing is 1.475 nm, the value of n_c/n_g can be got

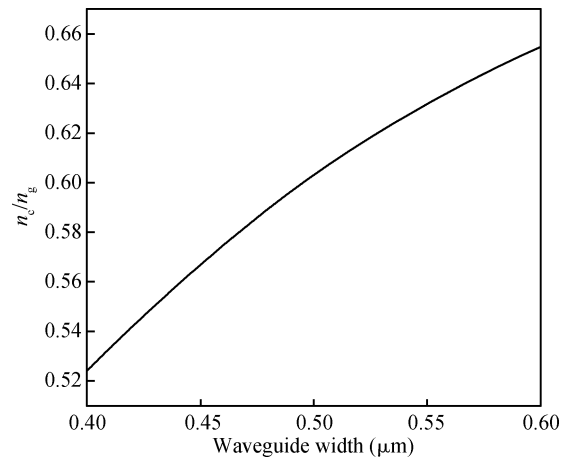


Fig. 5. Dependence of the ratio between the effective index n_c and the group index n_g (TE_0) with different widths.

from Eq. (5).

$$\frac{n_c}{n_g} = \frac{\Delta\lambda Rm}{\Delta x_0 n_s d} \approx 0.5635.$$

Thus, according to Fig. 5, the average waveguide width is about 446 nm. The calculated result is accordant with the measured result shown in Fig. 3(c). The change of the waveguide width must bring on the deviation of the central wavelength. The central wavelength can be calculated out from Eq. (2) and the value is 1487.5 nm. Due to the spectrum range of the emission source, it can not be demonstrated.

The factors which degrade our AWG's characteristic can be summarized as follows: systematic error and random error. The systematic error causes the width reduction of all waveguides, while the random error brings on the width fluctuation and the displacement of the channels separation. The systematic error and random error are both from mask error and dry etching during the fabrication process, so the enhancement of the related technology and the appropriate compensation method are necessary. For example, it can adapt the exposure dose partially to compensate the change of linewidth induced by the sloped sidewalls of waveguides in dry etching^[10].

4. Conclusion

A 16 channel 200 GHz arrayed waveguide grating based on Si nanowire waveguides with the crosstalk of 5–8 dB and the central channel's insertion loss of 2.2 dB is presented. For improving the device's performance, how to control the waveguide width in the large exposure area is a crucial factor. If the fabricated precision is fixed, broadening the waveguide width in the straight section of the arrayed region may bring substantial optimization^[9] and introducing the auxiliary waveguides in input/output/arrayed waveguide region is also a feasible method.

References

- [1] Claes T, Molera J G, De Vos K, et al. Label-free biosensing with a slot-waveguide-based ring resonator in silicon on insulator. *IEEE Photonics Journal*, 2009, 1(3): 197

- [2] Horst F, Green William M J, Offrein B J, et al. Echelle grating WDM (de-)multiplexers in SOI technology based on a design with two stigmatic points. SPIE, 2008, 6996: 69960R
- [3] Xiao Shijun, Khan M H, Shen Hao, et al. Multiple-channel silicon micro-resonator based filters for WDM applications. Optics Express, 2007, 15(12): 7489
- [4] Yamada H, Chu T, Ishida S, et al. Si photonic wire waveguide devices. IEEE J Sel Topics Quantum Electron, 2006, 12(6): 1371
- [5] Chen Yuanyuan, Li Yanping, Yu Jinzhong. A 4×4 thermo-optic SOI waveguide switch matrix. Journal of Optoelectronics Laser, 2009, 20(3): 283 (in Chinese)
- [6] Segawa T, Matsuo S, Kakitsuka T, et al. All-optical wavelength-routing switch with monolithically integrated filter-free tunable wavelength converters and an AWG. Optics Express, 2010, 18(5): 4340
- [7] Ahmad H, Zulkifli M Z, Latif A A, et al. Novel O-band tunable fiber laser using an array waveguide grating. Laser Phys Lett, 2010, 7(2): 164
- [8] Dai Daoxin, Liu Liu, Wosinski L, et al. Design and fabrication of ultra-small overlapped AWG demultiplexer based on α -Si nanowire waveguides. Electron Lett, 2006, 42(7): 400
- [9] Bogaerts W, Selvaraja S K, Dumon P, et al. Silicon-on-insulator spectral filters fabricated with CMOS technology. IEEE J Sel Topics Quantum Electron, 2010, 16(1): 33
- [10] Selvaraja S K, Bogaerts W, Dumon P, et al. Subnanometer linewidth uniformity in silicon nanophotonic waveguide devices using CMOS fabrication technology. IEEE J Sel Topics Quantum Electron, 2010, 16(1): 316